

Halo formation and self-pinch of an electron beam undergoing the Weibel instability

Vladimir Khudik, Igor Kaganovich, and Gennady Shvets

Citation: *Phys. Plasmas* **19**, 103106 (2012); doi: 10.1063/1.4759263

View online: <http://dx.doi.org/10.1063/1.4759263>

View Table of Contents: <http://pop.aip.org/resource/1/PHPAEN/v19/i10>

Published by the [American Institute of Physics](#).

Related Articles

Quantum ring solitons and nonlocal effects in plasma wake field excitations

Phys. Plasmas **19**, 102106 (2012)

Characteristics of ion-acoustic solitary wave in a laboratory dusty plasma under the influence of ion-beam

Phys. Plasmas **19**, 103704 (2012)

1.5D quasilinear model and its application on beams interacting with Alfvén eigenmodes in DIII-D

Phys. Plasmas **19**, 092511 (2012)

0.22 THz wideband sheet electron beam traveling wave tube amplifier: Cold test measurements and beam wave interaction analysis

Phys. Plasmas **19**, 093110 (2012)

A Vlasov equilibrium for space charge dominated beam in a misaligned solenoidal channel

Phys. Plasmas **19**, 080702 (2012)

Additional information on Phys. Plasmas

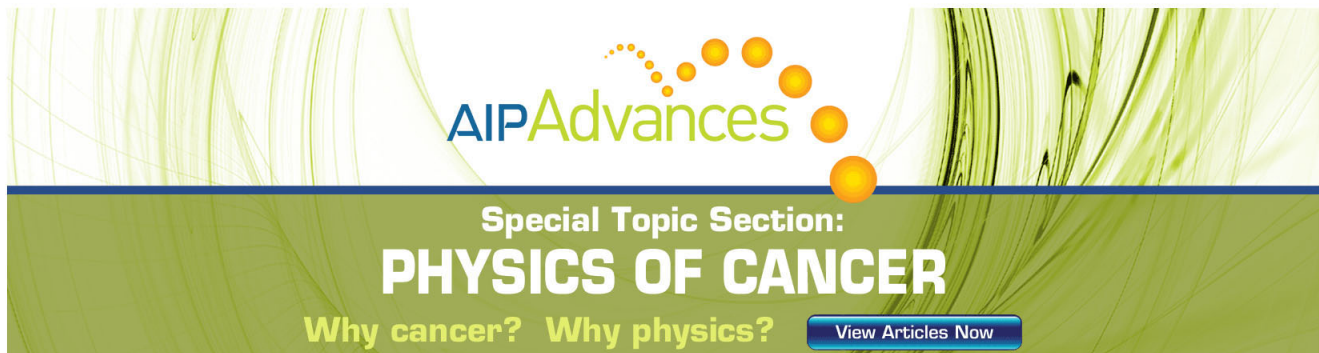
Journal Homepage: <http://pop.aip.org/>

Journal Information: http://pop.aip.org/about/about_the_journal

Top downloads: http://pop.aip.org/features/most_downloaded

Information for Authors: <http://pop.aip.org/authors>

ADVERTISEMENT



AIP Advances

Special Topic Section:
PHYSICS OF CANCER

Why cancer? Why physics? [View Articles Now](#)

Halo formation and self-pinching of an electron beam undergoing the Weibel instability

Vladimir Khudik,¹ Igor Kaganovich,² and Gennady Shvets¹

¹Department of Physics and Institute for Fusion Studies, The University of Texas at Austin, Texas 78712, USA

²Plasma Physics Laboratory, Princeton University, Princeton, New Jersey 08543, USA

(Received 6 July 2012; accepted 1 October 2012; published online 16 October 2012)

The collisionless Maxwellization of the energy distribution of an electron beam undergoing Weibel filamentation instability in a dense background plasma is demonstrated. While binary collisions between discrete charged particles are usually responsible for establishing the Maxwell-Boltzmann distribution (MBD) of non-equilibrium plasmas, we demonstrate that the same effect is achieved through collective collisions between multiple beam filaments. The final state of the filaments' merger is a single pinched beam surrounded by a wide halo. An analytic model for the equilibrated beam is developed and used to estimate spatial profiles of the pinched beam and its halo, the temperature, and the magnetic field. Results of analytical theory agree well with those of particle-in-cell simulations. Deviations from the MBD are explained by incomplete Maxwellization of the electrons with high and low transverse energies. © 2012 American Institute of Physics. [<http://dx.doi.org/10.1063/1.4759263>]

I. INTRODUCTION

The Weibel instability (WI)^{1–5} of plasmas with anisotropic velocity distribution (for example, relativistic electron beams propagating through the cold plasma) is one of the most basic and long-studied collective plasma processes. There has been a significant revival in theoretical studies of the WI because it is viewed as highly relevant to at least two areas of science: astrophysics of gamma-ray bursts (GRBs) and their afterglows^{6–11} and the fast ignitor¹² scenario of the inertial confinement fusion (ICF). Specifically, generation of the upstream magnetic field during GRB aftershocks is considered necessary for explaining emission spectra of the afterglows as well as for generating and sustaining collisionless shocks responsible for particle acceleration during GRBs. Collisionless Weibel instability is the likeliest mechanism^{6–11} for producing such magnetic fields. The WI is likely to play an important role in the fast ignitor scenario¹² because it can result in the collective energy loss of a relativistic electron beam in both coronal and core plasma regions.^{12–20}

The physics of the collisionless (i.e., with negligible binary collisions) WI is relatively well understood on qualitative level through particle-in-cell (PIC) simulations. The beam first breaks up into a large number of small filaments of transverse size $\approx \delta_p = c/\omega_p$, where $\omega_p = \sqrt{4\pi e^2 n_p/m}$ is the electron plasma frequency, n_p is the uniform background plasma density, and m and e are the electron mass and charge. The subsequent cascade of merging filaments results in a super-filament carrying the spatially compressed current of the original beam. The emergence and subsequent merger of beam filaments illustrated by Fig. 1 destroys the initial detailed balance between the beam current and plasma return current, and leads to magnetic field generation. Thus, the initial energy of directed motion of the beam is partially transferred to those of the magnetic field, transverse motion of the beam, and the plasma. What is missing from this

description is the analytic theory capable of quantitatively predicting some of the basic properties of the final state of the compressed beam: its spatial density profile, transverse temperature, and the amount of energy transferred to the magnetic field. Here, we present such a theory in the limit of small beam density $n_b \ll n_p$, transverse temperature $T/mc^2 \ll n_b/n_p$, and large initial area $L^2 \gg \delta_p^2$. Our numerical PIC simulations confirm the key assumption¹¹ of the theory developed below: that electron beam Maxwellization is achieved by filament merger, even in the absence of binary beam-plasma collisions.

II. MODEL DESCRIPTION

To make further analytic progress, we assume a two-dimensional ($x-y$) geometry that has been frequently used in previous computational studies,^{5,15,20,21} with the beam initially propagating in the uniform z -direction with the relativistic momentum $p_{b0} = \gamma_{b0} m v_{b0}$. Although a variety of electrostatic perturbations with finite k_z are excited by the beam, including the fast-growing oblique modes,^{22,23} we leave them outside of the scope of this work because of their much higher sensitivity to longitudinal and transverse plasma non-uniformities²⁴ compared with the more robust Weibel-type electromagnetic instabilities. Throughout the rest of the paper, all extensive quantities, such as particle number and field/particle energies, are defined per unit length in z . Plasma ions are assumed to be infinitely heavy forming a uniform background of density n_p . Under these assumptions, the beam's evolution occurs on a time scale $\Delta t \gg 1/\omega_p$ so that the background plasma electrons can be treated as a charge-neutralizing fluid with the density $n_e = n_p - n_b$ carrying the return current $J_p = -en_e v_{pz}$,²⁵ while the beam's electrons must be treated kinetically. The dominant electric and magnetic fields can be expressed in terms of the z -component of the vector potential ψ as $\vec{B}_\perp = -\vec{e}_z \times \vec{\nabla}_\perp \psi$, $E_z = -(1/c)\partial_t \psi$, and $\vec{E}_\perp = -(v_{pz}/c)\vec{\nabla}_\perp \psi$,

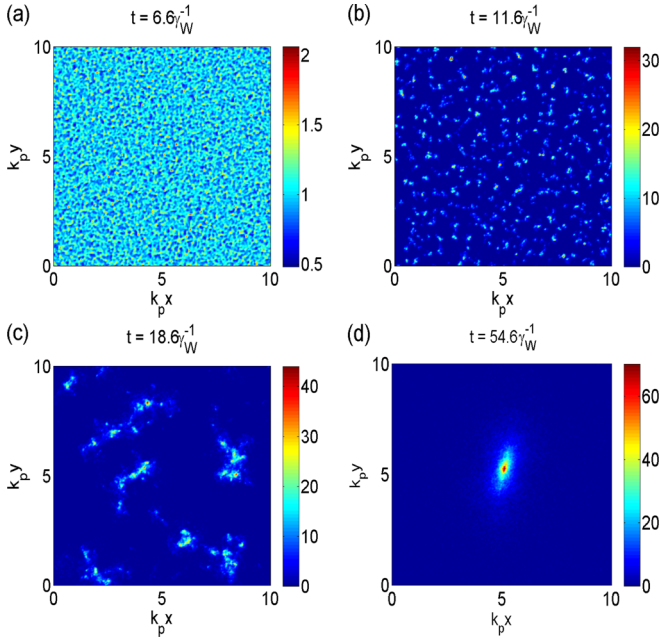


FIG. 1. Snapshots of the normalized density n_b/n_{b0} of a beam undergoing Weibel instability. The breakup of the initially uniform beam into a large number of non-stationary filaments (a) and (b) is followed by their merger (c) and eventual coalescence into a single quasi-stationary filament (d). The size of the compressed beam's core $r_B < \delta_p$, and over 30% of the beam's electrons are outside of the core, forming an extended halo. Initial beam parameters: $\gamma_b = 10$, $n_{b0} = 10^{-3}n_p$, $L = 10\delta_p$.

while the background plasma's motion primarily counters that of the beam: $v_{pz} = e\psi/mc$. The Ampere's Law is then expressed in the form of

$$\nabla_{\perp}^2 \psi - k_p^2(1 - n_b/n_p)\psi = -4\pi J_{bz}/c, \quad (1)$$

where J_{bz} is the beam's current and J_p is absorbed in the l.h.s. of Eq. (1). The relativistic dynamics of the individual (j^{th}) electron of the beam is described using the conservation of the canonical momentum, $\gamma_j v_{jz} = \gamma_{j0} v_{jz0} + e(\psi - \psi_0)/mc$, and the transverse equation of motion:

$$\frac{d(\gamma_j \vec{v}_{j\perp})}{dt} = -\frac{e(v_{jz} - e\psi/mc)}{mc} \vec{\nabla}_{\perp} \psi, \quad (2)$$

where ψ_0 is the initial magnetic potential in the plasma related to the plasma's initial velocity v_{z0} through $v_{z0} = e\psi_0/mc$. In the limit $n_b \ll n_p$ and $v_{jz} \approx -c$, $\gamma_j \approx \gamma_b$, plasma density depression and the radial electric field can be neglected and Eqs. (1) and (2) simplify to yield

$$\nabla_{\perp}^2 \psi - k_p^2 \psi = -4\pi e n_b, \quad m\gamma_b \frac{d\vec{v}_{j\perp}}{dt} = e\vec{\nabla}_{\perp} \psi. \quad (3)$$

According to Eq. (3), the beam's dynamics can be mathematically described as a pairwise interaction between the beam's electrons according to the screened gravitation-like attraction: the attraction energy between two current clumps $j_{bz}^{(k)}$ and $j_{bz}^{(l)}$ is given by $U_{kl} \propto -j_{bz}^{(k)} \times j_{bz}^{(l)} K_0(r_{kl}/\delta_p)$, where r_{kl} is the distance between the clumps, and K_0 is the modified Bessel function. Similar to the gravitational collapse of an interstellar cloud resulting in star formation,²⁶ the collapse

of an initially wide cold electron beam results in a smaller, hot beam filament of final radius r_B and temperature T .

However, as demonstrated below, there are several crucial differences between the beam collapse via WI and gravitational collapse of an interstellar cloud (or formally similar Bennett self-pinching²⁷ of a charge-neutralized electron beam). First, both r_B and T are determined primarily by the initial beam area L^2 , current I_b , and δ_p , and not by the initial beam temperature (which is assumed to vanish in this paper). Second, the WI-based compression of the beam does not proceed as a whole-beam compression. Instead, it starts from random current fluctuations and proceeds through filamentation and multiple filaments merger that gives rise to stochastic Maxwellization of the beam distribution function. Finally, screening of the potential ψ on the collisionless skin depth scale of δ_p results in the density profile of the compressed beam, which is very different from the textbook Bennett pinch equilibrium.²⁷ Another counter-intuitive consequence of the screening is that the area of the compressed filament $\propto r_B^2$ is *inversely proportional* to the initial beam area L^2 and always smaller than δ_p^2 . Such extreme compression is shown to be accompanied by an extensive particle halo outside of the compressed core that contains a large fraction of the beam's particles.

It follows from Eq. (3) that the effective transverse energy of the j^{th} electron is given by $\epsilon_{\perp j} = K_j - e\psi_j$, where $K_j = \gamma_j m v_{\perp j}^2/2$ is the transverse kinetic energy of an ultra-relativistic electron whose total energy can be expressed as $\gamma_j m c^2 \approx \gamma_j m v_{jz} c + K_j$. By defining the position-dependent transverse temperature of the beam as the momentum space average $\hat{T}(\vec{r}_{\perp}) \equiv \langle K_j \rangle$, the total energy conservation of the beam can be expressed as

$$U_{\perp} = \int n_b \hat{T} dA - \frac{1}{2} \int e n_b \psi dA = \text{const}, \quad (4)$$

where $dA = d^2 \vec{r}_{\perp}$. The potential energy given by the second term in the r.h.s. of Eq. (4) includes contributions of the magnetic field and plasma motion

$$-\frac{1}{2} \int e n_b \psi dA = -\frac{1}{8\pi} \int |\vec{B}_{\perp}|^2 dA - \frac{1}{2} \int n_p m v_{pz}^2 dA. \quad (5)$$

The negative sign of the potential energy²⁸ is responsible for the instability. Note that the consequence of the energy conservation $\Delta U_{\perp} = 0$ is that the total transverse energy gain of the beam is equal to the sum of the magnetic energy

$\Delta U_m = \int B^2/8\pi dA$ and the kinetic energy of the background plasma $\Delta U_p = \int n_p m (v_{pz}^2 - v_{0z}^2)/2 dA$.

III. ANALYTIC MODEL OF THE MODIFIED BENNETT PINCH

To quantify the parameters of the self-compressed filament, we assume the Maxwell-Boltzmann (MB) phase space distribution of the beam electrons $f(K, \vec{r}_{\perp}) \propto \exp(-K/T) \times \exp(e\psi/T)$, which implies the Boltzmann distribution of electron density: $n_b = n_{b*} \exp(e\psi/T)$. The constants n_{b*} and T are chosen to satisfy two conditions: (i) the total number of

electrons N and (ii) the total energy U_{\perp} in the final filament are the same as in the initial beam with the density n_{b0} and size L . Substituting n_b into Eq. (3) and assuming azimuthal symmetry yields

$$\frac{1}{\tilde{r}} \frac{d}{d\tilde{r}} \tilde{r} \frac{d}{d\tilde{r}} \left(\frac{\tilde{\psi}}{\tilde{T}} \right) = \frac{\tilde{\psi}}{\tilde{T}} - \frac{n_{b^*}/n_{b0}}{\tilde{T}} \exp\left(\frac{\tilde{\psi}}{\tilde{T}}\right). \quad (6)$$

The dimensionless (tilded) quantities are normalized according to $\tilde{r} = r/\delta_p$ and $(\tilde{\psi}, \tilde{T}) = (e\psi, T)/\epsilon_0$, where $\epsilon_0 = (n_{b0}/n_p)mc^2$. Equation (6) can be solved numerically by choosing $\tilde{\psi}(0) \equiv e\psi_{\max}/\epsilon_0$ and \tilde{T} satisfying (i) and (ii). Moreover, in the limit of a highly self-compressed beam with characteristic size $r_B \ll \delta_p$, approximate semi-analytic expressions for the filament's temperature can be obtained

$$T \approx \frac{mc^2/2}{1 + W(\alpha_0 L^2/\delta_p^2)} \frac{I_b}{I_{A0}}, \quad (7)$$

where $I_b = en_{b0}cL^2$ is the total beam current, $I_{A0} = mc^3/e$ is the non-relativistic limiting Alfvén current, $W(x)$ is the Lambert W-function (defined as $W \exp(W) = x$), and $\alpha_0 = 0.0341$. The filament's effective size r_B is given by $r_B^2 \approx 5(\delta_p^4/L^2)W[\alpha_0(L/\delta_p + A_1)^2]$, where $A_1 = 35$ is a numerical factor, can be used to conveniently express the beam's density distribution in and around the filament

$$n_b \approx n_{b0} \frac{8\delta_p^2/r_B^2}{(1 + r^2/r_B^2)^2} \tilde{T} + n_{b\infty}, \quad (8)$$

as well as the magnetic potential produced by the filament: $\tilde{\psi} \approx 4\tilde{T}K_0[(r^2 + r_B^2)^{1/2}/\delta_p] + \tilde{\psi}_{\infty}$. Here $n_{b\infty}$ and $\tilde{\psi}_{\infty}$ are the density and the potential far away from the filament center.

The halo density around the filament, $n_{b\infty}/n_{b0} \approx \alpha_1(r_B^2/\delta_p^2)\tilde{T}$ ($\alpha_1 = \exp 4\gamma_E \approx 5$, where γ_E is the Euler constant), is one of the distinguishing features of the modified Bennett pinch given by Eq. (8). Note that the standard Bennett pinch²⁷ given by the first term in the r.h.s. of Eq. (8) does not possess a halo because its magnetic potential ψ diverges logarithmically at $r = \infty$. To our knowledge, Eqs. (7) and (8) rep-

resent the first analytic theory of the modified Bennett pinch which develops self-consistently in the presence of the Weibel instability of an initially cold electron beam. They provide quantitative predictions of the size of the self-compressed beam filament's core $r_B < \delta_p$, the degree of density compression $n_b(r=0)/n_{b0}$, and the amount of halo electrons outside of the dense filament's core. For the examples presented below, a very significant fraction of the beam's electrons (as high as 1/3) are in the halo region.

IV. SIMULATION RESULTS

To check the validity of the key assumption of the beam's Maxwellization, we have carried out 2D simulations of Eqs. (1) and (2) in the domain $L \times L = 10\delta_p \times 10\delta_p$ with grid spacings $\Delta x = \Delta y = L/256 \approx 0.04\delta_p$ and periodic boundary conditions in both directions x and y , by using PIC code developed earlier.^{19,25} The Helmholtz equation was solved by the multigrid method, and a numerical heating was avoided by implementing energy conserving algorithm.²⁹ The initial beam density was $n_{b0} = 10^{-3}n_p$, and relativistic factor $\gamma_{b0} = 10$. The time sequence of the emergence of multiple small filaments and their subsequent merger is shown in Fig. 1. After $t \sim 31\gamma_W^{-1}$ (where $\gamma_W = \omega_p\beta_z\sqrt{n_{b0}/\gamma_b n_p}$ is the typical growth rate of the WI^{3-6,9,16,19}), filaments' merger eventually results in a single quasi-stationary elliptical filament undergoing slow rotation. In agreement with the analytic model, the filament consists of a dense core surrounded by an extended halo.

The electron distribution as a function of the total transverse electron energy with respect to the minimum of the potential well $\psi_{\max} = \psi(r=0)$ (defined as $\epsilon_{\text{tot}} = K - e(\psi - \psi_{\max})$) obtained from PIC simulations is shown in Fig. 2(a). Indeed, the majority of electrons are distributed according to the MB distribution (MBD: straight line) with temperature $T_{\text{PIC}} \approx 1.9\epsilon_0$. This temperature is in good agreement with the analytically predicted $T_{\text{an}} \approx 1.88\epsilon_0$. Maxwellization of beam's electrons is accomplished through stochastic inelastic collisions between multiple current filaments acting as macro-particles; it does not require binary collisions between individual beam or plasma particles.

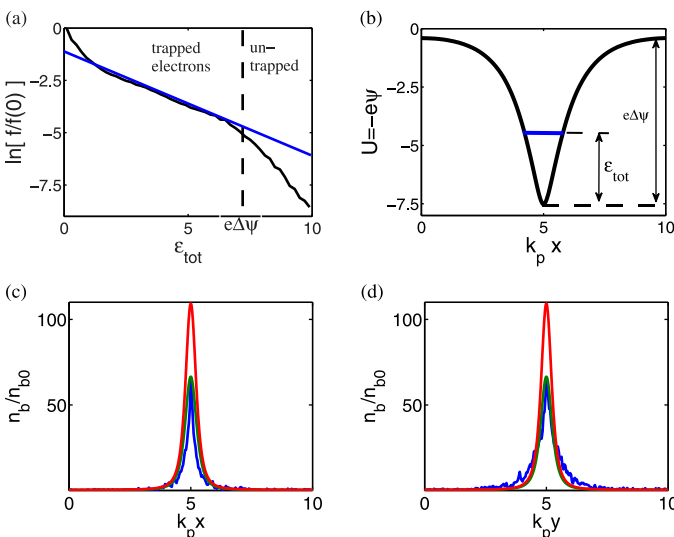


FIG. 2. (a) The beam electron distribution $\ln[f/f(0)]$ as a function of ϵ_{tot} (in units of ϵ_0). Blue line corresponds to the Maxwellian distribution with $T = T_{\text{PIC}} = 1.9\epsilon_0$. (b) Potential well formed by the vector potential: particles are trapped when $\epsilon_{\text{tot}} < e\Delta\psi$ and untrapped when $\epsilon_{\text{tot}} > e\Delta\psi$. (c) and (d) Beam density distribution in x and y cross sections (blue) from PIC simulations compared to that in the modified Bennett pinch with $T = T_{\text{an}}$ (red) and $T = T_{\text{fil}}$ (green).

Noticeable deviations from the MBD for deeply trapped (low energy) and untrapped (high-energy: $\epsilon_{\text{tot}} > e\Delta\psi$, where $\Delta\psi \equiv \psi_{\text{max}} - \psi_{\infty}$ as illustrated in Fig. 2(b)) electrons can be observed in Fig. 2(a). These two classes of electrons do not experience a sufficient number of thermalizing filament mergers either because of their peripheral location, or because they are quickly trapped inside one of the larger filaments. Specifically, the number of filament mergers experienced by the un-trapped electrons is not sufficient to boost their energy beyond $\epsilon_{\text{tot}} > 7.2\epsilon_0$.

Similarly, low energy electrons are confined to the center of the filament and do not experience the time-dependent magnetic field during filaments' merger. Therefore, the effective temperature $T_{\text{fil}} \approx 1.3\epsilon_0$ obtained numerically by averaging over all electrons in the filament, is somewhat lower than T_{an} . The physical implication of the incomplete Maxwellization of this electron population is a somewhat reduced compression ratio $n_b(r=0)/n_{b0}$ of the final filament's core. Figures 2(c) and 2(d) show the comparison of the analytic density profiles given by Eq. (8), with $T = T_{\text{an}}$ and $T = T_{\text{fil}}$, to those extracted from the PIC simulation (lineouts along the x and y axis, respectively). Clearly, choosing $T = T_{\text{fil}}$ results in a better agreement between theory and simulations. Note that the filament's radius r_B weakly depends on the temperature, and the agreement between the analytically predicted radius $r_b^{\text{an}} = 0.37\delta_p$ and that from PIC simulations $r_b^{\text{PIC}} = 0.40\delta_p$ is very close.

With the assumptions of the analytic theory validated, we can now estimate the average energy loss of the longitudinal energy by a relativistic electron beam undergoing self-compression. Using $U_{\perp} \approx 0$, we find that the energy transferred from the beam longitudinal motion, $\langle \Delta(\gamma_b mc^2)_{\parallel} \rangle \approx -2T$, is repartitioned between the beam's transverse energy NT (where N is the number of beam's electrons), kinetic energy increase of the background plasma ΔU_p , and the magnetic field's energy ΔU_m according to the following scalings:

$$\Delta U_m \approx 2NT \frac{1.3r_B/\delta_p - \ln(r_B/\delta_p) - 0.88}{1 + W(\alpha_0 L^2/\delta_p^2)} \quad (9)$$

and $\Delta U_p = NT - \Delta U_m$. For the parameters of the PIC simulations depicted in Figs. 1 and 2, the analytic prediction of the ra-

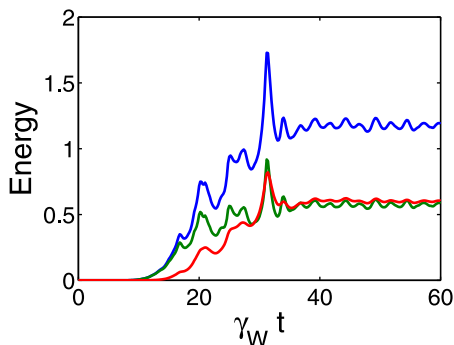


FIG. 3. The evolution of the transverse kinetic energy of beam particles (blue), the magnetic energy (green), and the energy of plasma particles (red). The energy is measured in units $\epsilon_0 N$, where N is the number particles in the beam.

tio between magnetic and plasma kinetic energies is $\Delta U_m = 0.52NT$ and $\Delta U_p = 0.48NT$. This repartition ratio is in agreement with the results of PIC simulations, shown in Fig. 3.

V. SUMMARY

In summary, an analytical model describing the self-pinching of a relativistic charge-neutralized electron beam undergoing the collisionless Weibel instability in an overdense plasma has been developed. The model accurately predicts the final temperature and size of the self-focused filament. It is found that the final temperature is primarily defined by the total beam's current, while the filament's radius is shown to be smaller than the collisionless skin depth in the plasma and primarily determined by the beam's initial size. The model also accurately predicts the repartitioning ratio of the initial energy of the beam's forward motion into the magnetic field energy and the kinetic energy of the surrounding plasma. The density profile of the final filament is shown to be a superposition of the standard Bennett pinch profile and a wide halo surrounding the pinch, which contains a significant fraction of the beam's electrons. PIC simulations confirm the key assumption of the analytic theory: the collisionless merger of multiple current filaments in the course of the Weibel Instability provides the mechanism for Maxwellization of the beam's distribution function. Deviations from the Maxwell-Boltzmann distribution are explained by incomplete thermalization of the deeply trapped and halo electrons. It is conjectured that the simple expression derived here can be used for understanding collisionless^{11,22} shock acceleration and magnetic field amplification in astrophysical plasmas.

One of the interesting questions left out of the scope of this paper is the detailed dynamics of the beam merger and self-pinching. It is clear that for a very large initial transverse area of the beam, interaction between separate filaments becomes weak at the late stages of the merging, and many factors (e.g., initial conditions, collisions between plasma electrons and ions, inhomogeneity of the density in the halo) influence the merging process.

ACKNOWLEDGMENTS

This work was supported by the US DOE Grant Nos. DE-FG02-05ER54840 and DE-FG02-04ER41321. We thank E. Startsev for fruitful discussions.

¹E. W. Weibel, *Phys. Rev. Lett.* **2**, 83 (1959).

²B. D. Fried, *Phys. Fluids* **2**, 337 (1959)

³R. L. Morse and C. W. Nielson, *Phys. Fluids* **14**, 830 (1971).

⁴R. C. Davidson, D. A. Hammer, I. Haber, and C. E. Wagner, *Phys. Fluids* **15**, 317 (1972).

⁵R. Lee and M. Lampe, *Phys. Rev. Lett.* **31**, 1390 (1973).

⁶M. V. Medvedev and A. Loeb, *Astrophys. J.* **526**, 697 (1999).

⁷M. V. Medvedev, M. Fiore, R. A. Fonseca, L. O. Silva, and W. B. Mori, *Astrophys. J.* **618**, L75 (2005).

⁸A. Gruzinov, *Astrophys. J.* **563**, L15 (2001).

⁹L. O. Silva, R. A. Fonseca, J. W. Tonge, W. B. Mori, and J. M. Dawson, *Phys. Plasmas* **9**, 2458 (2002).

¹⁰M. Milosavljevic, E. Nakar, and A. Spitkovsky, *Astrophys. J.* **637**, 765 (2006).

¹¹A. Spitkovsky, *Astrophys. J.* **673**, L39 (2008).

- ¹²M. Tabak, J. Hammer, M. E. Glinsky, W. L. Kruer, S. C. Wilks, J. Woodworth, E. M. Campbell, M. D. Perry, and R. J. Mason, *Phys. Plasmas* **1**, 1626 (1994).
- ¹³J. J. Honrubia and J. Meyer-ter-Vehn, *Nucl. Fusion* **46**, L25 (2006).
- ¹⁴S. Atzeni and J. Meyer-ter-Vehn, *The Physics of Inertial Fusion* (Oxford University Press, New York, 2004), p. 409.
- ¹⁵T. Taguchi, T. M. Antonsen, Jr., C. S. Liu, and K. Mima, *Phys. Rev. Lett.* **86**, 5055 (2001).
- ¹⁶R. A. Fonseca, L. O. Silva, J. W. Tonge, W. B. Mori, and J. M. Dawson, *Phys. Plasmas* **10**, 1979 (2003).
- ¹⁷V. M. Malkin and N. J. Fisch, *Phys. Rev. Lett.* **89**, 125004 (2002).
- ¹⁸J. M. Hill, M. H. Key, S. P. Hatchett, and R. R. Freeman, *Phys. Plasmas* **12**, 082304 (2005).
- ¹⁹O. Polomarov, A. B. Sefkow, I. Kaganovich, and G. Shvets, *Phys. Plasmas* **14**, 043103 (2007).
- ²⁰M. Honda, J. Meyer-ter-Vehn, and A. Pukhov, *Phys. Rev. Lett.* **85**, 2128 (2000).
- ²¹O. Polomarov, I. Kaganovich, and G. Shvets, *Phys. Rev. Lett.* **101**, 175001 (2008).
- ²²A. Bret, L. Gremillet, and M. E. Dieckmann, *Phys. Plasmas* **17**, 120501 (2010).
- ²³A. Bret, M.-C. Firpo, and C. Deutsch, *Phys. Rev. Lett.* **94**, 115002 (2005).
- ²⁴B. N. Breizman, *Reviews of Plasma Physics* (Consultants Bureau, London, NY, 1990), Vol. 15, pp. 61–162).
- ²⁵G. Shvets, O. Polomarov, V. Khudik, C. Siemon, and I. Kaganovich, *Phys. Plasmas* **16**, 056303 (2009).
- ²⁶D. Prialnik, *An Introduction to the Theory of Stellar Structure and Evolution* (Cambridge University Press, 2000), p. 195212.
- ²⁷R. C. Davidson, *Physics of Nonneutral Plasmas* (Addison-Wesley, 1990), p. 122.
- ²⁸A. Karmakar, N. Kumar, G. Shvets, O. Polomarov, and A. Pukhov, *Phys. Rev. Lett.* **101**, 255001 (2008).
- ²⁹C. K. Birdsall and A. B. Langdon, *Plasma Physics via Computer Simulation* (Institute of Physics, 2005), p. 213.